Turbulence measurements using Doppler backscattering system during $\rho*$ and $\nu*$ scans on Tore Supra

L. Vermare[1], P. Hennequin[1], Ö. D. Gürcan[1], C. Bourdelle[2], F. Clairet[2], G. Falchetto[2], C. Fenzi[2], R. Sabot[2], M. Schubert[2], J.L. Segui[2] and the Tore Supra Team

[1] *Ecole Polytechnique, LPP, CNRS UMR 7648,91128 Palaiseau, France*

[2] *CEA, IRFM, F-13108 Saint-Paul-lez-Durance, France*

Introduction

Particle and heat transport induced by micro-turbulence play a crucial role in tokamak performance. The understanding of turbulent transport in the core tokamak plasmas requires detailed comparison between theoretical models and experimental measurements of turbulence. One effective method for validating transport models across different tokamaks is to use a dimensionless description of plasma dynamics. With this in mind, new $\nu*$ and $\rho*$ scans have been performed on Tore Supra,with the objective of combining transport and turbulence measurements, including theory-experiment comparison. The Tore Supra tokamak is particularly well suited to perform such experiments due to long discharge operation. This provides long stationary phases allowing comfortable transport analysis and turbulence measurements, which improves statistics and/or resolution. In addition, it is equipped with complementary microwave diagnostics to measure density fluctuations. The present paper focuses on the shape of the perpendicular wavenumber spectrum obtained using Doppler backscattering system during both $\rho*$ and $\nu*$ scans.

Doppler backscattering system on Tore Supra

Taking advantage of both scattering and reflectometry techniques, Doppler backscattering is based on the possibility to separately detect the field backscattered on fluctuations along the beam path from the field reflected at the cut-off layer (standard reflectometry) [1, 2, 3]. In this technique, the probing beam is launching in oblique incidence with respect to the cutoff layer. Fluctuations whose wave-number matches the Bragg rule are selected $\vec{k}_f = -2\vec{k}_i$, where $\vec{k}_i$ is the local probing wave-vector. The probing beam wave-vector is determined by the angle α to the normal to the iso-index layer: at the cut-off $k_i = k_0 sin\alpha$ (slab geometry) where k_0 is the vacuum wave-number. The localized swelling of the incident field near the cut-off amplifies the scattering process close to the cut-off layer : incident radial k_r vanishes at the cut-off while the fluctuation wave-number spectrum is concentrated at small k_r [4, 5, 6]. This technique thus provides the instantaneous spatial Fourier transform of density fluctuations, $\tilde{n}(\vec{k},t) = \int_V n(\vec{r},t)e^{i\vec{k}\vec{r}}d\vec{r}$, with a band pass filter in k-space around $k = 2k_0 sin\alpha$ near the cut-off layer. The frequency spectrum obtained by this technique is Doppler shifted as $\Delta\omega = k_\perp v_\perp$ where $v_\perp$ is the perpendicular fluctuation velocity in the laboratory frame.

The Doppler backscattering system installed on Tore Supra is composed of two channels, one in O-mode polarization in the V-band range (50-75GHz) the second one in X-mode polarization in the W-band (75-110GHz). Probing is done from the tokamak low-field side. Gaussian beams

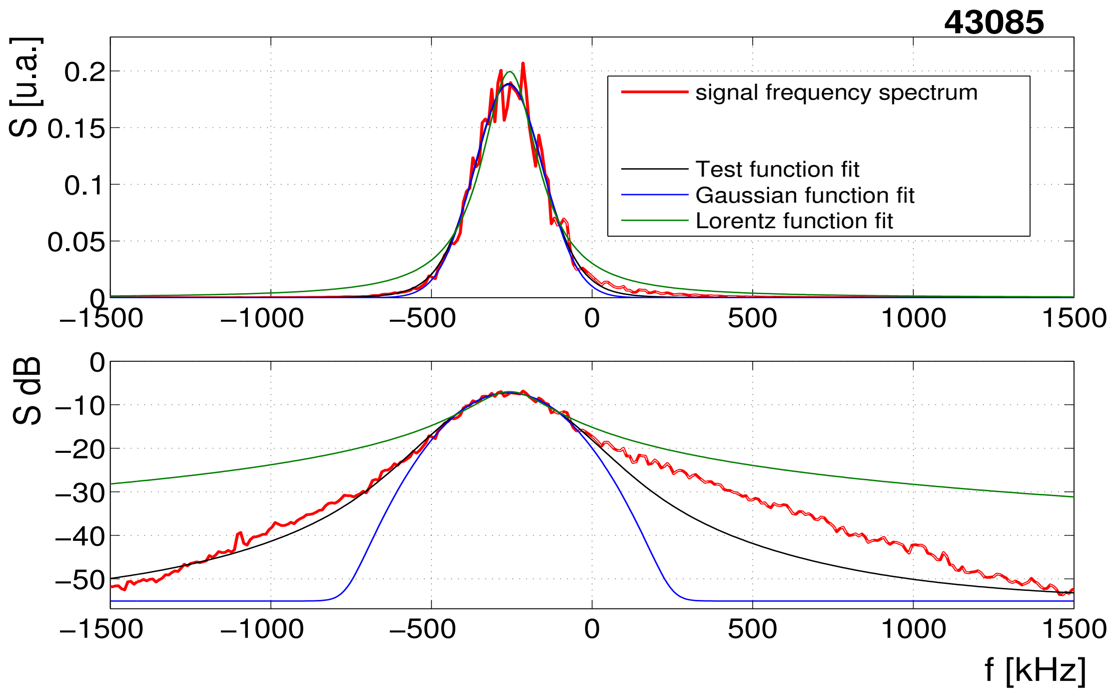

Figure 1: Frequency spectrum at $r/a =$ and k_θ. Fitting functions : Gaussian function in green, Lorentz function in blue and test function in black

are used (beam divergence 2.2. HPBW) and the motorized antenna is tiltable from -1^o to 10^o ($\alpha = -3^o : 20^o$) during the discharge. 3D ray tracing code with Gaussian beam propagation [7] is used to evaluate the reflection layer radius r (turning point) from where the scattered signal is expected to come and k at this reflection layer. For each pair (F,θ), the measured frequency spectrum (figure 1) is fitted using a Gaussian, a Lorentzian or the test function as shown in the figure 1 [8]. In the whole core region, the Doppler shift is generally negative corresponding to fluctuations moving in the electron diamagnetic direction.

Principle of k-spectrum measurements using Doppler backscattering system

The turbulence amplitude is extracted from the frequency spectrum of the scattered signal: the density of power spectrum of the scattering signal at a specific k is evaluated by integrating the Doppler frequency spectrum. The integrations are performed using the best fit functions in order to separate the Doppler component from the additional f = 0 component. As illustrated in figure 1, the best fit corresponds to the test function, which is neither a Gaussian nor a Lorentzian , but a generalization of the two. Scanning the tilt angle θ changes the probed wave-number k and allows us to build a k-spectrum. Obtaining a k-spectrum at fixed radius requires combined (F,θ) scans since changing θ also changes the turning point location. Indeed, during the stationary phase of a discharge, several sets of frequency steps are programmed (e.g. 10 steps require less than 200 ms) while the antenna tilt angle is swept (the angle sweep is sufficiently slow to ensure that the angle does not change much during the acquisition time).

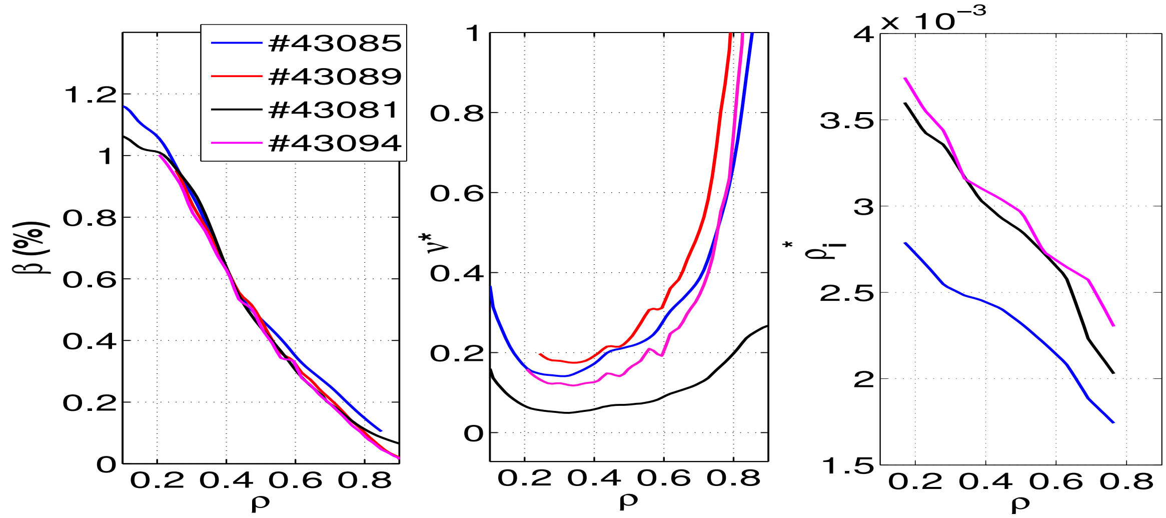

Figure 2: radial profiles of the dimensionless paramaters β, ν^* and ρ^* during both ρ^* and ν^* scans.

The scattered power is then corrected from the incident beam power variation with the probing frequency. However note that here we have assumed that the scattering efficiency does not vary much with the tilt angle in this k range, i.e. that the scattered power is proportional to $\left|\tilde{n}(\vec{k}_\perp)\right|^2$.

Description of the experiments

Dedicated scans of dimensionless parameters are performed by varying the magnetic field (B) from one discharge to another and adjusting the plasma current (Ip), density (ne) and temperature ($T_{e,i}$) in order to keep the other dimensionless parameters constant. For example, to scan ρ^*, the temperature has to vary as $B^{2/3}$ and the density as $B^{4/3}$. Following these requirements, ρ^* varies as $B^{-2/3}$ constraining strongly the range over which ρ^* can be scanned in a given machine. During a ν^* scan, the density must be kept constant, while the temperature should be varied as B^2, which makes ν^* change as B^{-4} . Thus, it is easier to cover a large range in ν^*. Tore Supra experiments were performed in L-mode plasmas (hence without interfering with H-mode edge physics). The temperature was changed using ICRH heating using H-minority scheme, for which the frequency was adjusted according to the magnetic field in order to keep a central deposition. The density profiles were determined using fast sweep reflectometry, the electron temperature profiles were measured by electron cyclotron emission radiometer and ion temperature profiles were obtained from charge exchange recombination spectroscopy measurements.

In the first scan, $\nu^* = \nu_{ei}/\varepsilon\omega_{be}$ has been varied from $\nu^* = 0.16$ to $\nu^* = 0.56$ by changing the magnetic fields from B=3.8T to B=2.8T. This scan is complementary to a previous one [9] performed in a higher range of $\nu^* = [0.16 - 0.7]$ (lower additional power). Radial profiles of the dimensionless parameters β, ρ_i^* and ν^* are plotted in figure 2 and show a good matching of ρ_i^* (less than 15% mismatch) and β (less than 10% mismatch) between the selected three discharges (43081, 43089/43094) inside $\rho = [0.2 - 0.8]$. Note that during these scans, the

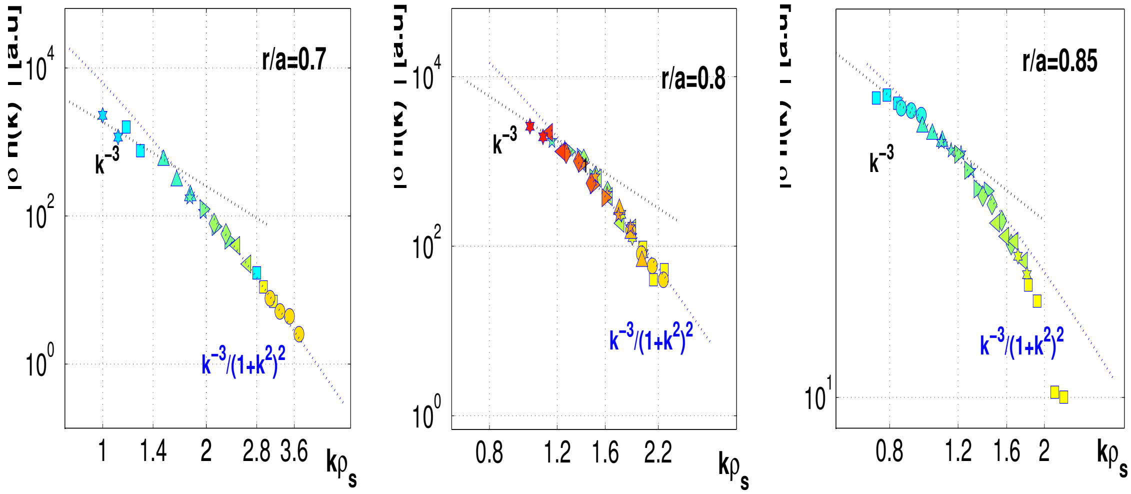

Figure 3: perpendicular wavenumber spectra during (from the left to the rigth) the discharges 43081, 43089 and 43085

discharge 43094 is similar to the discharge 43089 in which no Ti measurements were avalaible.

Concerning the ρ^* scan, in order to cover the largest possible range of ρ^* values, the magnetic field has been varied from 3.8T to 2.1T corresponding to $\rho_e^* = [4-6.2]e^{-5}$. However in this present paper only $3.8T$ and $2.8T$ are presented which correspond to $\rho_e^* = [4-4.7]e^{-5}$ (43085 and 43089/43094).

Results

For each discharge, turbulence measurements and local analysis were performed over a long stationary phase characterized by a time window Δt larger than 1s. Perpendicular wavenumber spectra, measured during the three discharges using O-mode channel are plotted in figure 3. Note that in O mode, the selected wave number at the cut-off is mainly in $\hat{b} \times \hat{r}$ direction. The radial window width is $r/a \pm 0.05$. The wave-number selectivity Δk is related to the scattering volume and thus to the antenna pattern [3, 6] and varies from $\pm 1.1 cm^{-1}$ to $\pm 1.8 cm^{-1}$ during these discharges. However, decreasing the step size of the tilt angle ($\approx 0.6^o$) allows us to describe k-spectrum with a resolution in k around $0.5 cm^{-1}$. The spectral shape is similar to previous observations on Tore Supra during ohmic discharges using a scattering diagnostic [10], (ICRH power in the present discharges go up to 5MW). At low k, the spectrum shape is compatible with a power law with a spectral index ≈ -3 [1, 11, 12]. This behavior has been compared against gyrokinetic simulations and found to be in fair agreement between $k\rho_s = 0.5-1$ [13]. At higher k, this power law representation breaks, as previously observed from the CO2 laser scattering experiment [14].

We also compared the measured poloidal wavenumber spectra with $k^{-3}/(1+k^2)^2$, which corresponds to the spectrum of drift wave turbulence when the disparate scale interactions are dominant [15]. The results show a reasonably good agreement except for the discharge 43085 (low ρ^* case), in which the experimental spectrum decreases faster at high k

In addition, changing ν^* by more than a factor 4 or ρ^* (factor 1.6) does not affect the shape of the poloidal wavenumber spectrum in the gradient zone (around $r/a = 0.7 - 0.9$). The deviation for the power law k^{-3} appears for the three discharge between $k\rho_s = [1 : 1.5]$.

This work was carried out within the framework the European Fusion Development Agreement (EFDA) and the French Research Federation for Fusion Studies (FR-FCM). It is supported by the European Communities under the contract of Association between Euratom and CEA. The views and opinions expressed herein do not necessarily reflect those of the European Commission. Financial support was also received from Agence Nationale de la Recherche under contract ANR-06-BLAN-0084

References

[1] X.L. Zou, et al., 26th EPS Conf. on Controlled Fusion and Plasma Phys. (1999) vol 23J p 1041
[2] V. Bulanin V. et al., Plasma Phys. Rep. (2000) 26 813
[3] M. Hirsch et al., Rev. Sci. Instrum. (2001) 72 324
[4] X.L. Zou et al., Proc. 4th Reflectometry Workshop (1999) EUR-CEA-1674
[5] E.Z. Gusakov et al., 28th EPS Conf. on Controlled Fusion and Plasma Phys. (2001) vol 25A p 361
[6] V. Bulanin V., etal., 29th EPS Conf. on Controlled Fusion and Plasma Phys. (2002) vol 26B P2.121
[7] C. Honore et al., Nucl. Fusion 46 (2006) S809
[8] P. Hennequin P. et al., 26th EPS Conf. on Controlled Fusion and Plasma Phys. (1999) P 3.006 p 977
[9] T. Gerbaud et al., 35rd EPS Conf. on Controlled Fusion and Plasma Phys. (2008)
[10] P. Hennequin P. et al., Nucl. Fusion 46 (2006) S771
[11] P. Devynck et al., Plasma Phys. Control Fusion 35 (1993) 63
[12] D.L. Brower D.L., W.A Peebles and N.C Luhmann, Nucl. Fusion 27 (1987) 2055
[13] A. Casati at al., Phys. Rev. Letter 102 (2009) 165005
[14] P. Hennequin et al., Plasma Phys. Control. Fusion 46 (2004) B121
[15] O. Gurcan at al., Phys. Rev. Letter 102 (2009) 255002